Faculty of Mathematical Sciences

University of Twente
The Netherlands

P.O. Box 217
7500 AE Enschede
The Netherlands
Phone: +31-53-4893400
Fax: +31-53-4893114
Email: memo@math.utwente.nl
www.math.utwente.nl/publications

Memorandum No. 1649

Performance analysis of downlink shared channels in a UMTS network

R. Litjens[1] and R.J. Boucherie

October, 2002

ISSN 0169-2690

[1]Knowledge Innovation Center, KPN Research, The Netherlands

PERFORMANCE ANALYSIS OF DOWNLINK SHARED CHANNELS IN A UMTS NETWORK

Remco Litjens
Knowledge Innovation Center, KPN Research, The Netherlands
Tel: +31 70 446 3419, Fax: +31 70 446 3477, E-mail: R.Litjens@kpn.com

Richard J. Boucherie*
Faculty of Mathematical Sciences, University of Twente, The Netherlands
Tel: +31 53 489 3432, Fax: +31 53 489 3069, E-mail: R.J.Boucherie@math.utwente.nl

ABSTRACT

In light of the expected growth in wireless data communications and the commonly anticipated up/downlink asymmetry, we present a performance analysis of downlink data transfer over Downlink Shared CHannels (DSCHs), arguably the most efficient UMTS transport channel for medium-to-large data transfers. It is our objective to provide qualitative insight in the different aspects that influence the data Quality Of Service (QOS). As a most principal factor, the data traffic load affects the data QOS in two distinct manners: *(i)* a heavier data traffic load implies a greater competition for DSCH resources and thus longer transfer delays; and *(ii)* since each data call served on a DSCH must maintain an Associated Dedicated CHannel (A-DCH) for signalling purposes, a heavier data traffic load implies a higher interference level, a higher frame error rate and thus a lower effective aggregate DSCH throughput: *the greater the demand for service, the smaller the aggregate service capacity*. The latter effect is further amplified in a multicellular scenario, where a DSCH experiences additional interference from the DSCHs and A-DCHs in surrounding cells, causing a further degradation of its effective throughput. Following an insightful two-stage performance evaluation approach, which segregates the interference aspects from the traffic dynamics, a set of numerical experiments is executed in order to demonstrate these effects and obtain qualitative insight in the impact of various system aspects on the data QOS.

Keywords: UMTS, Downlink Shared CHannel, mobile data communications, processor sharing models, scheduling, performance evaluation, Markov chain analysis.

AMS subject classifications. Primary: 90B18, 90B22. Secondary: 60K25.

1 INTRODUCTION

Wireless data transfer is undisputedly a major driver for the deployment and anticipated success of third-generation mobile networks such as the Universal Mobile Telecommunications System (UMTS) [5, 10]. As the foreseen (data) services greatly differ in their traffic characteristics and QOS requirements, a number of distinct transport channels have been specified to accomodate these services most efficiently [1, 10]. In the UMTS downlink, the focus of our attention in light of the generally expected strong up/downlink data traffic asymmetry, the Dedicated CHannel (DCH), the Forward Access CHannel (FACH) and the Downlink Shared CHannel

*The research of Richard J. Boucherie is partly supported by the Technology Foundation STW, applied science division of NWO and the technology programme of the Ministry of Economic Affairs, The Netherlands.

(DSCH) are standardised. Specifically designed for delay-sensitive services or services with stringent throughput requirements, the DCH is a 'bit pipe' assigned exclusively to a single Mobile Station (MS) and has the advantage of fast closed-loop power control and macro-diversity. On the other hand, the FACH and DSCH may be shared by multiple MSs. The FACH is typically used for the transfer of relatively small data chunks, without the advantages of closed-loop power control and macro-diversity. Medium- to large data transfers, particularly of bursty character (e.g. TCP/IP flows), are most efficiently conveyed on the DSCH, as it enjoys the advantages of closed-loop power control by maintaining a low bit rate Associated DCH (A-DCH) for each data call to carry control signalling information. A principal advantage is the enhanced efficiency of channelization code usage. Since data is multiplexed on the DSCHs, the use of soft handover (or macro-diversity) is rather complicated from an implementation viewpoint and therefore not standardised.

The data Quality Of Service (QOS) is influenced by the data traffic load in two distinct manners. The most obvious *'round robin effect'* is that under a heavier data traffic load, the given DSCH service rate is typically shared by a larger number of competing data calls so that an individual data call receives less attention from the DSCH server and hence the experienced QOS is worse. On the other hand, the *'interference effect'* comprises of a reduced effective DSCH throughput as an increasing number of data calls and hence A-DCHs raises the interference levels and thus the DSCH frame error rate: the greater the demand for service, the smaller the aggregate service capacity. The latter effect is further amplified in a multicellular scenario, where a DSCH experiences additional interference from the DSCHs and A-DCHs in surrounding cells, causing a further degradation of its effective throughput.

Contribution and outline The presented study provides qualitative insight in the different system and traffic aspects that affect the DSCH performance in UMTS networks. In particular, we are interested in the specific impact of the above-mentioned 'round robin' and 'interference effects' on the data QOS under different data traffic loads. As the downlink orthogonality factor, i.e., the degree of non-orthogonality among signals generated by the same BTS, influences the balance between intra- and intercellular interference, the sensitivity of the QOS with respect to this propagation environment-specific system parameter is also determined. A two-stage modelling approach is presented to segregate the interference aspects from the traffic dynamics. This segregation supports an insightful analysis of the relevant system aspects.

The outline of the paper is as follows. Section 2 provides a brief review of the related literature. Section 3 describes the model under investigation, while Section 4 presents the evaluation approach in terms of a decomposition of the general model into distinct experiments. The two-stage performance analysis of each experiment is outlined in Section 5. Subsequently, Section 6 presents a set of demonstrative numerical experiments and discusses the results. Section 7 ends the paper with some concluding remarks and aims for further research.

2 LITERATURE

Most performance studies for CDMA-based networks have traditionally focussed on speech-only networks. Only in the last few years researchers have shifted their focus to data-only and integrated services networks, in line with the technology-driven system evolutions. Given the commonly anticipated traffic asymmetry, virtually all recent data QOS investigations focus on downlink data transfer.

Purely *analytical* studies in this field appear complicated and are therefore rare. One noteworthy example is [3], which identifies optimality properties for downlink scheduling in linear CDMA-based data networks. It is proven that if the self-orthogonality factor is smaller (better) than the cross-orthogonality factor (across distinct signals generated by the same BTS), one-by-one scheduling outperforms simultaneous data transfers (on a per BTS basis). Note that this result advocates the use of shared (e.g. DSCHs) rather than dedicated channels (DCHs) for data transfer. In [4] an equivalent proof of the optimality of one-by-one scheduling over

code-multiplexing (simultaneous transfers) is given, which is subsequently exploited to conclude that one-by-one scheduling minimises total transfer time as well as the required energy. In [12] the rate processor sharing scheduling algorithm is presented and evaluated for the downlink of a single CDMA cell, which is equivalent to the widely adopted generalised processor sharing scheme in wireline networking. As in the investigations presented in this paper, a useful separation between the queueing and wireless aspects is made by characterising each user by a so-called effective weight, i.e., the amount of power required to support a unit data rate. Given these weights, queueing analysis is applied to determine the scheduling weights required to meet delay targets, and to determine rules for call admission control. Using analysis in combination with Monte Carlo techniques, [15, 16] quantify the performance gain that can be achieved by efficiently up- and downgrading of DSCH data rates in support of a varying presence of prioritised speech calls. It is demonstrated that such adaptive scheduling can enhance both speech outage probabilities and data throughputs.

Among the published *simulation* studies that have recently focused on data scheduling in CDMA-based networks, we refer to [2, 9, 11, 19]. [2] presents an extensive simulation study of nine different rate- and delay-based scheduling algorithms for the downlink of a (single) data-only CDMA cell, concentrating on the relevant tradeoffs between efficiency and fairness. Another extensive simulation-based comparison of scheduling schemes is presented in [11]. In light of the primary advantage of DSCH deployment of saving spreading codes and its main disadvantage of not allowing macro-diversity, [9] propose and evaluate a hybrid scheme that serves remote data users on DCHs with the benefits of macro-diversity and near users on a DSCH. [19] compare a round robin and a C/I-based scheduling scheme, as well as a hybrid form of these schemes, via simulations, where the hybrid scheme is shown to be as fair as pure round robin, while providing higher throughputs. C/I-based scheduling provides high system throughput but poor fairness. The last three references ([9, 11, 19]) consider a multicellular network.

Note that, with the exception of [19], none of the papers that either implicitly or explicitly concentrate on the DSCH performance, includes the potentially significant effects of the A-DCHs. Furthermore, some of the papers leave out the impact of intercellular interference caused by DSCH and A-DCH transmissions, focussing on single cell systems. The semi-analytical performance evaluation approach presented here is therefore applied to provide qualitative insight in the (relative) significance of these system aspects.

3 MODEL

This section sets the framework for the presented performance analysis by describing the system, interference and traffic models in generic terms. Concrete parameter settings are specified in Table 1 at the beginning of Section 6 below.

System model Consider a UMTS network of B hexagonal cells with radius R served by omnidirectional Base Transceiver Stations (BTSs) (see Figure 1). In light of the anticipated dominance of wireless data services and the expected up-/downlink data traffic load asymmetry, the presented investigation concentrates on the modelling and performance evaluation of UMTS's Downlink Shared CHannel (DSCH), a transport channel specifically designed to convey (bursty) downlink data traffic in a resource efficient manner. The system model assumes the deployment of a single DSCH with a given nominal bit rate R_{DSCH} at each BTS $b \in \mathbb{B} \equiv \{1, 2, \cdots, B\}$ and E_b/N_o target γ_{DSCH}, which multiplexes the present data calls according to an idealised round robin scheduling discipline. Each data call that is served on the DSCH maintains a low bit rate Associated Dedicated CHannel (A-DCH) for control signalling purposes, a.o. to support closed-loop power control. The A-DCHs are characterised by bit rate $R_{\text{A-DCH}}$ and E_b/N_o target $\gamma_{\text{A-DCH}}$. The closed-loop power control maintained on the A-DCH enables power

efficient DSCH transmissions, by applying a fixed DSCH/A-DCH power offset of

$$p_{\text{DSCH}} : p_{\text{A-DCH}} = \frac{\gamma_{\text{DSCH}} R_{\text{DSCH}}}{R_{\text{CHIP}}} : \frac{\gamma_{\text{A-DCH}} R_{\text{A-DCH}}}{R_{\text{CHIP}}} \Longleftrightarrow p_{\text{DSCH}} = p_{\text{A-DCH}} \left(\frac{\gamma_{\text{DSCH}} R_{\text{DSCH}}}{\gamma_{\text{A-DCH}} R_{\text{A-DCH}}} \right), \tag{1}$$

where R_{CHIP} denotes the system chip rate, γ_{DSCH} ($R_{\text{DSCH}}/R_{\text{CHIP}}$) is the DSCH's C/I target, and $\gamma_{\text{A-DCH}}$ ($R_{\text{A-DCH}}/R_{\text{CHIP}}$) is the A-DCH's C/I target. Such a fixed power offset can be applied because the DSCH and the A-DCH transmissions share the same propagation paths from the serving BTS to the MS, and hence experience identical path gain variations. Although in general DCHs allow the use of soft handover to enhance radio link quality and resource efficiency, this feature does not apply to the A-DCHs as it would preclude the proper use of a fixed DSCH/A-DCH power offset for DSCH power control (recall that the DSCH does not support soft handover). The BTS's (downlink) transmission power budget is denoted $p_{\max}$.

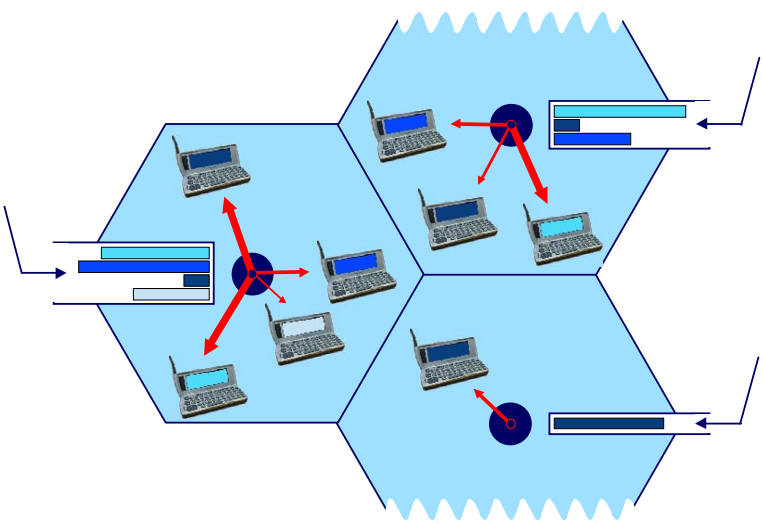

Figure 1: *System model* ($B = 3$).

Interference model The radio propagation model considers a single signal path with correlated lognormal shadowing and Rayleigh fading. Given a distance r between the transmitter BTS and the receiver MS, the relation between transmission ($p_{\text{transmission}}$) and the instantaneous reception ($p_{\text{reception}}$) power (in Watt) is given by

$$p_{\text{reception}} = p_{\text{transmission}} \cdot \mathcal{G}_{\text{MS BTS}} = p_{\text{transmission}} \cdot \eta_{\text{basic}} \cdot r^{-\varsigma} \cdot 10^{(a\xi_{\text{MS}} + b\xi_{\text{BTS}})/10} \cdot \zeta_{\text{Rayleigh}},$$

where η_{basic} reflects the basic transmission loss, ς is the path loss exponent, $a\xi_{\text{MS}} + b\xi_{\text{BTS}}$ is the correlated shadowing effect (in dB), with ξ_{MS}, $\xi_{\text{BTS}} \sim N\left(0, \sigma_{\text{S}}^2\right)$ the MS- and BTS-specific shadowing effects and a and b the correlation factors [23], and $\zeta_{\text{Rayleigh}} \sim Exp\,(1)$ the random (instantaneous) Rayleigh fading effect (e.g. [13]). $\zeta_{\text{Rayleigh}}^{-1} \mathcal{G}_{\text{MS BTS}}$ gives the local average of the path gain between the considered MS and BTS, which is used to assign a serving BTS to a given MS. In C/I calculations, ω denotes the downlink orthogonality factor, reflecting the degree of orthogonality of signals generated by the same BTS, assumed to be the same for time-shifted versions of identical or different signals from the same BTS. The value of ω typically depends on the propagation environment. The spatially uniform thermal noise level is denoted $\nu > 0$.

Traffic model The considered UMTS network serves data calls only, assumed to be downlink transfers of files with exponentially distributed sizes. The mean file size is denoted μ^{-1} (in kbits). File transfer requests are generated according to a Poisson process with rate λ_b in cell $b \in \mathbb{B}$, and terminals are uniformly distributed over the cell of origination. Note that a data call originating in cell $b \in \mathbb{B}$ (i.e., geographically nearest to BTS b) may be nearer (in the path gain sense) to BTS $b' \neq b$ due to the shadowing effects. Without loss of generality

this effect is assumed to be captured by the λ_b's, so that λ_b is the average arrival rate of data calls that are nearest (in the path gain sense) to BTS $b \in \mathbb{B}$. Let $\rho_b \equiv \lambda_b / (\mu R_b)$ denote the (normalised) data traffic load in cell $b \in \mathbb{B}$. Two distinct Call Admission Control (CAC) thresholds are enforced. Firstly, an MS whose location (read: local average path gain) is so unfortunate that its C/I requirement cannot be met even in an otherwise empty system, i.e.,

$$\max_{b \in \mathbb{B}} \zeta_{\text{Rayleigh}}^{-1} \mathcal{G}_{\text{MS } b} < \frac{\nu}{\left(\frac{R_{\text{CHIP}}}{\gamma_{\text{DSCH}} R_{\text{DSCH}} + \gamma_{\text{A-DCH}} R_{\text{A-DCH}}} - \omega \right) p_{\max}}, \tag{2}$$

is rejected in order to avoid serving 'hopeless' calls. In the above path gain threshold, which is derived using (1), the term '$\gamma_{\text{A-DCH}} R_{\text{A-DCH}}$' should be omitted if no A-DCHs are considered. The second CAC threshold limits the number of data jobs in service to $a_{\max}$ in each cell in order to provide some minimum QOS, so that the space of feasible system states is given by

$$\mathbb{S} \equiv \left\{ \mathbf{a} \equiv (a_1, a_2, \cdots, a_B) \in \{0, \cdots, a_{\max}\}^B \right\},$$

where a_b denotes the number of data calls in cell $b \in \mathbb{B}$. Let $\mathbb{S}_b^+ \equiv \{\mathbf{a} \in \mathbb{S} : a_b > 0\}$ denote the set of states in which at least one data call is served at BTS $b \in \mathbb{B}$. The setting of the CAC threshold $a_{\max}$ is addressed in Section 5 and demonstrated in Section 6 below. In principle, the presented analysis allows the CAC decision to be less myopic and also include the actual loading at e.g. adjacent cells, but for our qualitative purposes we chose to keep the CAC scheme simple.

4 EVALUATION APPROACH

In order to obtain the intended qualitative insight regarding the 'round robin effect' and the 'interference effects' of the traffic load on the DSCH performance, the general framework described in the previous section is decomposed into five distinct experiments, as visualised in Figure 2. The most basic EXPERIMENT 0 considers a single BTS (and DSCH) without any interference or other radio interface-specific effects and thus captures the 'round robin effect'. The different 'interference effects' are captured by the subsequent experiments. EXPERIMENT 1A adds the DSCH's self-interference due to orthogonality loss, while EXPERIMENT 1B further adds the interference from the maintained A-DCHs, still considering a single BTS. The impact of the inter-BTS interference from the DSCH and A-DCHs is investigated by adding additional BTSs in EXPERIMENTs 2 and 3. Although the evaluation method readily extends to an arbitrary numbr of BTSs, the largest network size is set to three BTSs in order to allow reasonably swift analytical calculations.

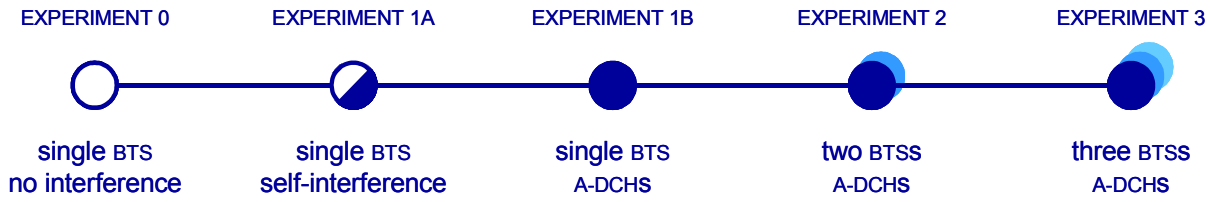

Figure 2: *Illustration of evaluation approach.*

5 PERFORMANCE ANALYSIS

The principal objective of this section is to outline the performance analysis required for EXPERIMENTs 2 and 3, including all relevant system aspects, while the specific characteristics of the simpler EXPERIMENTS 0-1 are discussed in a separate paragraph at the end of each subsection.

As in a CDMA-based network, the precise locations of the served calls have a significant impact on the required transmission powers, the corresponding interference levels, the induced Frame Error Rates (FERs) and hence the

experienced throughputs, the performance evaluation approach generally encountered in similar models, is that of (time-consuming) dynamic system-level simulations. Given our qualitative objective to generate insight in the DSCH performance and its sensitivity to e.g. the presence of the A-DCHs, the data traffic load and the downlink orthogonality factor, we propose a hybrid approach in two stages, which segregates the interference aspects from the traffic dynamics (along similar lines as followed in [8, 12]).

- In STAGE I a Monte Carlo simulation experiment is carried out to determine the outage probability that a reference call in cell $b \in \mathbb{B}$ experiences during its DSCH transfer as a function of the number of calls in each cell and *conditional* on its admission by the path gain-based CAC criterion (2). The set of outage probability functions is denoted $\left\{P_b(\mathbf{a}),\ \mathbf{a} \in \mathbb{S}_b^+,\ b \in \mathbb{B}\right\}$, and captures the random effects of terminal location and signal fading. The Monte Carlo simulations are also readily utilised to determine the fraction of calls $\mathbf{P}^{\mathcal{G}}$ that fails to satisfy the minimum path gain requirement and is thus rejected.

- STAGE II captures the traffic dynamics of call arrivals and terminations in a B-dimensional irreducible continuous-time Markov chain $(\mathbf{A}(t))_{t\geq 0} \equiv (A_1(t), A_2(t), \cdots, A_B(t))_{t\geq 0}$ with system states $\mathbf{a} \in \mathbb{S}$, specified by the effective cell-specific call arrival rates $\lambda_b\left(1-\mathbf{P}^{\mathcal{G}}\right)$ for a given gross fresh call arrival rate λ_b, $b \in \mathbb{B}$, the CAC threshold $a_{\max}$, and the expected effective throughput per data call given by

$$\beta_b(\mathbf{a}) \equiv a_b^{-1}\left(1-P_b(\mathbf{a})\right) R_{\text{DSCH}},$$

  as experienced in cell b in system state $\mathbf{a} \in \mathbb{S}$. Note that we may indeed apply the reduced arrival process with rate $\lambda_b\left(1-\mathbf{P}^{\mathcal{G}}\right)$ to the considered Markov chain, as it is is still Poisson due to the random filtering of badly located calls. Data scheduling is assumed to be done according to the processor sharing discipline, which is an idealised and analytically more tractable version of the round robin discipline. Here the outage probability functions obtained in STAGE I are interpreted as the experienced FERs. The data QOS can be derived from the equilibrium and transient behavior of the Markov chain.

Both stages are treated in more detail below.

STAGE I: INTERFERENCE ASPECTS

In STAGE I the set of functions $\left\{P_b(\mathbf{a}),\ \mathbf{a} \in \mathbb{S}_b^+,\ b \in \mathbb{B}\right\}$ is determined by means of Monte Carlo simulations, including the derivation of the CAC threshold $a_{\max}$ which bounds $\mathbb{S}_b$, $b \in \mathbb{B}$. For each feasible system state $\mathbf{a} \in \mathbb{S}_b^+$, K independent constellations (or snapshots) $(\mathbb{A}, \mathbb{D}, \mathcal{G}, \mathbf{b})_k$ are generated, $k = 1, \cdots, K$. Let $A \equiv \left(\sum_{b\in\mathbb{B}} a_b\right)$ denote the total number of data calls in the network in a given state $\mathbf{a} \in \mathbb{S}_b^+$. A constellation is specified by the set of all data calls $\mathbb{A} \equiv \{1, \cdots, A\}$, the subset $\mathbb{D} \subset \mathbb{A}$ of data calls that are (randomly) selected (one per non-idle BTS) for service by the round robin scheduler in the considered constellation, the $(A \times B)$-dimensional path gain matrix $\mathcal{G}$, and the A-dimensional base station assignment vector $\mathbf{b} \equiv (b_1, \cdots, b_A)$, where b_m denotes the BTS serving data call $m \in \mathbb{A}$, with $|\{m \in \mathbb{A} : b_m = b\}| = a_b$, $b \in \mathbb{B}$. In light of the path gain-based CAC criterion the Monte Carlo experiments are designed to ensure that the sampled data calls satisfy the minimum dominant path gain requirement (2).

In order to determine whether any of the active data calls experiences an outage in a given constellation $(\mathbb{A}, \mathbb{D}, \mathcal{G}, \mathbf{b})$[1], it is necessary to verify whether a vector $\mathbf{p} \equiv ((\widetilde{p}_m, m \in \mathbb{A}),\ (\widehat{p}_m, m \in \mathbb{D}))$ of A-DCH and DSCH

[1] For enhanced readability, the index k indicating the considered constellation will be omitted in the remainder of this section.

transmission powers exists, respectively, which satisfies the signals' C/I requirements:

$$\begin{cases} \dfrac{\widetilde{p}_m \mathcal{G}_{mb_m}}{\sum\limits_{m' \in \mathbb{A}} \omega\left(b_m, b_{m'}\right) \widetilde{p}_{m'} \mathcal{G}_{mb_{m'}} + \sum\limits_{m' \in \mathbb{D}} \omega\left(b_m, b_{m'}\right) \widehat{p}_{m'} \mathcal{G}_{mb_{m'}} + \nu} \geq \dfrac{\gamma_{\text{A-DCH}} R_{\text{CHIP}}}{R_{\text{A-DCH}}} & m \in \mathbb{A} \quad \text{(A-DCHs)} \\ \dfrac{\widehat{p}_m \mathcal{G}_{mb_m}}{\sum\limits_{m' \in \mathbb{A}} \omega\left(b_m, b_{m'}\right) \widetilde{p}_{m'} \mathcal{G}_{mb_{m'}} + \sum\limits_{m' \in \mathbb{D}} \omega\left(b_m, b_{m'}\right) \widehat{p}_{m'} \mathcal{G}_{mb_{m'}} + \nu} \geq \dfrac{\gamma_{\text{DSCH}} R_{\text{CHIP}}}{R_{\text{DSCH}}} & m \in \mathbb{D} \quad \text{(DSCHs)} \\ \sum\limits_{m \in \mathbb{A}: b_m = b} \widetilde{p}_m + \sum\limits_{m \in \mathbb{D}: b_m = b} \widehat{p}_m \leq p_{\max} & b \in \mathbb{B} \quad \text{(power budget)} \end{cases}$$

where

$$\omega\left(b, b'\right) \equiv \begin{cases} \omega & \text{if } b = b' \\ 1 & \text{if } b \neq b' \end{cases}$$

gives the appropriate the downlink orthogonality factor.

We refer to [15] for the details of determining the Pareto-optimal power vector that satisfies the above system of inequalities if it is feasible, or the suboptimal power vector in case it is infeasible and all C/I's in the congested cell(s) are proportionally downgraded to meet the power budget restriction(s). Whether or not any of the DSCHs experiences an outage can be determined immediately from the achieved (sub)optimal power vector. It is noted that even if the system as a whole is not feasible, possibly due to one congested cell, it is possible that the DSCH C/I target is satisfied in some, more lightly loaded, cells sufficiently far from the bottleneck cell(s).

Performance measures If for a given system state $\mathbf{a} \in \mathbb{S}_b^+$, BTS b's DSCH experienced an outage in $o_b\left(\mathbf{a}\right)$ out of K snapshots, the outage probability is estimated at

$$P_b\left(\mathbf{a}\right) \equiv \frac{o_b\left(\mathbf{a}\right)}{K}, \ b \in \mathbb{B}.$$

The outage probability functions $\left\{P_b\left(\mathbf{a}\right), \ \mathbf{a} \in \mathbb{S}_b^+, \ b \in \mathbb{B}\right\}$ are increasing in R_{DSCH}, due to the more demanding C/I requirements, and decreasing in ω, due to the reduced experienced interference. As the $P_b\left(\mathbf{a}\right)$'s are specified for a given realisation of the system state, they do not depend on the traffic dynamics. Note that the obtained set of functions $\left\{P_b\left(\mathbf{a}\right), \ \mathbf{a} \in \mathbb{S}_b^+, \ b \in \mathbb{B}\right\}$, with $P_b\left(\mathbf{a}\right)$ increasing in each a_b, $b \in \mathbb{B}$, implicitly indicates the amount of resources that a data call at a given BTS claims at all other BTSs in terms of a reduced effective DSCH throughput, and is in that sense similar to the effective interference models that have been derived for DCHs in CDMA-based networks (see e.g. [8, 14]). The CAC threshold $a_{\max}$ is derived from the obtained outage probability functions in combination with an operator's target value, thereby effectively bounding $\mathbb{S}_b$ (and hence $\mathbb{S}_b^+$), for each $b \in \mathbb{B}$.

Other experiments The STAGE 1 Monte Carlo analyses required to obtain the outage probabilities of the simpler experiments are considerably less extensive than that needed for the most complete EXPERIMENT 3. Recall that the basic reference EXPERIMENT 0 excludes all radio interface-related aspects and therefore requires no results from STAGE 1 ($\mathbf{P}^{\mathcal{G}} = P_1\left(a_1\right) = 0, \ a_1 \in \mathbb{S}_1^+$). The outage probability in EXPERIMENT 1A is influenced merely by whether the considered DSCH is on or off, and not by the *number* of present data calls, due to the absence of A-DCHs. Therefore only a single outage probability $P_1^{\star}\left(1\right)$ is required, while the A-DCH related C/I requirements are redundant in determining whether the reference DSCH experiences an outage in a given constellation. The analysis for EXPERIMENT 1B is equivalent to that for EXPERIMENTS 2 and 3, requiring $a_{\max}$ outage probabilities $\left\{P_1\left(a_1\right), \ a_1 \in \mathbb{S}_1^+\right\}$.

STAGE II: TRAFFIC DYNAMICS

Given the outage probability functions $\left\{P_b\left(\mathbf{a}\right),\ \mathbf{a}\in\mathbb{S}_b^+,\ b\in\mathbb{B}\right\}$ obtained via Monte Carlo simulations in STAGE I and the selected CAC threshold $a_{\max}$, it is the objective of STAGE II to derive the desired performance measures by incorporating these interference-related aspects with the traffic dynamics in a Markovian analysis. Interpreting the outage probability as the FER, the expected effective DSCH throughput per data call offered by BTS $b\in\mathbb{B}$ in system state $\mathbf{a}\in\mathbb{S}_b^+$ is given by

$$\beta_b\left(\mathbf{a}\right)\equiv a_b^{-1}\left(1-P_b\left(\mathbf{a}\right)\right)R_{\text{DSCH}}.$$

Along with the Poisson call arrival rates and the exponentially distributed file sizes, the system evolution can be described by the continuous-time Markov chain $\left(\mathbf{A}(t)\right)_{t\geq 0}\equiv\left(A_1(t),A_2(t),\cdots,A_B(t)\right)_{t\geq 0}$ with states denoted $\mathbf{a}\in\mathbb{S}$. The Markov chain's infinitesimal generator, denoted $\mathcal{Q}$, is defined by

$$\mathcal{Q}(\mathbf{a},\mathbf{a}')=\begin{cases}\lambda_b\left(1-\mathbf{P}^{\mathcal{G}}\right) & \text{if } \mathbf{a}'=\mathbf{a}+\mathbf{e}_b\\ \mu a_b\beta_b\left(\mathbf{a}\right) & \text{if } \mathbf{a}'=\mathbf{a}-\mathbf{e}_b\end{cases}$$

for $\mathbf{a},\mathbf{a}'\in\mathbb{S}$, where $\mathbf{e}_b$ is the B-dimensional vector with all zeroes, except a one on position b, and $\mathbf{P}^{\mathcal{G}}$ denotes the fraction of calls that fails to satisfy the minimum path gain requirement (2). All other non-diagonal entries of $\mathcal{Q}$ are 0, while the diagonal entries are such that all rows of $\mathcal{Q}$ sum up to 0. Since the finite state space Markov chain $\left(\mathbf{A}(t)\right)_{t\geq 0}$ is irreducible, a unique probability vector $\boldsymbol{\pi}$ exists that satisfies the system of global balance equations:

$$\boldsymbol{\pi}\mathcal{Q}=\mathbf{0},$$

with $\mathbf{0}$ the vector with all entries zero. For $B>1$, no closed-form expression for $\boldsymbol{\pi}$ is known, due to the influence of $a_{b'}$, $b'\neq b$, on the DSCH throughput at BTS b. Therefore, numerical methods, e.g. the successive overrelaxation method (see [22]) are applied to determine the equilibrium distribution.

Performance measures A number of basic performance measures can be obtained directly from the equilibrium distribution. From a system's perspective, the (cell-specific) expected channel utilisation expresses the achieved resource efficiency, while the Grade Of Service is readily termed in terms of the overall (cell-specific) data call blocking probabilities (using the PASTA property [24]):

$$\mathbf{P}_b\equiv\mathbf{P}^{\mathcal{G}}+\left(1-\mathbf{P}^{\mathcal{G}}\right)\sum_{\{\mathbf{a}\in\mathbb{S}:a_b=a_{\max}\}}\pi\left(\mathbf{a}\right)\quad\text{and}\quad\mathbf{P}\equiv\sum_{b\in\mathbb{B}}\left(\frac{\lambda_b}{\sum_{b'\in\mathbb{B}}\lambda_{b'}}\right)\mathbf{P}_b,$$

which include the effects of *both* CAC conditions. Of principal relevance in the presented investigation is the experienced data QOS, expressed as the (cell-specific) expected transfer time $\mathbf{T}$ ($\mathbf{T}_b$, $b\in\mathbb{B}$) of a data call, which is readily derived applying Little's formula:

$$\mathbf{T}_b\equiv\frac{\mathbf{N}_b}{\lambda_b\left(1-\mathbf{P}_b\right)}=\frac{\sum_{\mathbf{a}\in\mathbb{S}}a_b\,\pi\left(\mathbf{a}\right)}{\lambda_b\left(1-\mathbf{P}_b\right)},\ b\in\mathbb{B},$$

and

$$\mathbf{T}\equiv\sum_{b\in\mathbb{B}}\left(\frac{\lambda_b\left(1-\mathbf{P}_b\right)}{\sum_{b'\in\mathbb{B}}\lambda_{b'}\left(1-\mathbf{P}_{b'}\right)}\right)\mathbf{T}_b=\frac{\sum_{\mathbf{a}\in\mathbb{S}}\left(\sum_{b\in\mathbb{B}}a_b\right)\pi\left(\mathbf{a}\right)}{\left(\sum_{b\in\mathbb{B}}\lambda_b\right)\left(1-\mathbf{P}\right)},$$

where $\mathbf{N}_b$ denotes the expected number of data calls in cell $b\in\mathbb{B}$.

Aside from the above performance measures which can be obtained directly from the Markov chain's equilibrium distribution, the expected transfer time $\widehat{\tau}_b(\mathbf{a},x)$ of a data call admitted to BTS $b\in\mathbb{B}$ can be determined conditional on the state $\mathbf{a}\in\mathbb{S}_b^+$ of the system upon call arrival (where a_b includes the new data call) and on the data call size $x\in\mathbb{R}^+$. Since the derivation follows the same analytical lines as presented in [17, 21], we merely

state the result here. Let $\mathcal{Q}_b^\star$ denote the infinitesimal generator of the modified version of the original Markov chain $(\mathbf{A}(t))_{t\geq 0}$ characterised by the presence of one permanent data call in cell $b \in \mathbb{B}$, i.e.

$$\mathcal{Q}_b^\bullet(\mathbf{a},\mathbf{a}') = \begin{cases} \lambda_{b'}\left(1-\mathbf{P}^{\mathcal{G}}\right) & \text{if } \mathbf{a}' = \mathbf{a}+\mathbf{e}_{b'} \\ \mu\left(a_b-1\right)\beta_b\left(\mathbf{a}\right) & \text{if } \mathbf{a}' = \mathbf{a}-\mathbf{e}_b \\ \mu a_{b'}\beta_{b'}\left(\mathbf{a}\right) & \text{if } \mathbf{a}' = \mathbf{a}-\mathbf{e}_{b'} \text{ with } b' \neq b \end{cases}$$

for $\mathbf{a},\mathbf{a}' \in \mathbb{S}_b^+$. All other non-diagonal entries of $\mathcal{Q}_b^\bullet$ are 0, while the diagonal entries are such that all rows of $\mathcal{Q}_b^\bullet$ sum up to 0. The permanent data call, i.e., the tagged call whose transfer time is to be determined, never leaves the system, but shares in the varying DSCH throughput as if it were finite. Let $\boldsymbol{\pi}_b^\bullet$ be the stationary probability distribution vector corresponding to the modified Markov chain, i.e. $\boldsymbol{\pi}_b^\bullet \mathcal{Q}_b^\bullet = \mathbf{0}$. Furthermore, let $\mathcal{B}_b \equiv diag(\beta_b(\mathbf{a}),\ \mathbf{a} \in \mathbb{S}_b^+)$ denote the diagonal matrix of expected effective DSCH throughputs per data call. Then the closed-form solution for $\widehat{\boldsymbol{\tau}}_b(x) \equiv \left(\widehat{\tau}_b(\mathbf{a},x),\ \mathbf{a} \in \mathbb{S}_b^+\right)$ is then given by

$$\widehat{\boldsymbol{\tau}}_b(x) = \frac{x}{\boldsymbol{\pi}_b^\bullet \mathcal{B}_b \mathbf{1}}\mathbf{1} + \left[\mathcal{I} - \exp\left\{x\mathcal{B}_b^{-1}\mathcal{Q}_b^\bullet\right\}\right]\boldsymbol{\gamma}_b,$$

where $\boldsymbol{\gamma}_b \equiv \left(\gamma_b\left(\mathbf{a}\right),\ \mathbf{a} \in \mathbb{S}_b^+\right)$ is the unique solution to the system of linear equations

$$\begin{aligned} \mathcal{Q}_b^\bullet \boldsymbol{\gamma}_b &= \frac{\mathcal{B}_b\mathbf{1}}{\boldsymbol{\pi}_b^\star \mathcal{B}_b \mathbf{1}} - \mathbf{1}, \\ \boldsymbol{\pi}_b^\bullet \mathcal{B}_b \boldsymbol{\gamma}_b &= 1. \end{aligned}$$

The conditional expected transfer time of a data call of size x served by BTS b is then given by

$$\mathbf{T}_b\left(x\right) \equiv \sum_{\mathbf{a}\in\mathbb{S}_b^+} \widehat{\tau}_b(\mathbf{a},x)\left(\frac{\pi\left(\mathbf{a}-\mathbf{e}_b\right)}{\sum_{\mathbf{a}'\in\mathbb{S}_b^+}\pi\left(\mathbf{a}'-\mathbf{e}_b\right)}\right),$$

where $\mathbf{e}_b$ is the B-dimensional vector with a one on the b^{th} position and zeroes elsewhere.

Other experiments The performance analyses for EXPERIMENTs 0 and 1A are similar to those of EXPERIMENTs 2 and 3 presented above. The only difference is that the expected effective DSCH throughput per data call $\beta_b\left(\mathbf{a}\right)$ offered by BTS $b \in \mathbb{B} = \{1\}$ in system state $\mathbf{a} \in \mathbb{S}_b^+$, is now given by

$$\beta_b\left(\mathbf{a}\right) \equiv \begin{cases} a_b^{-1} R_{\text{DSCH}} & (\text{EXPERIMENT } 0), \\ a_b^{-1}\left(1-P_b^\star\left(1\right)\right)R_{\text{DSCH}} & (\text{EXPERIMENT } 1\text{A}). \end{cases}$$

Whereas the multi-BTS EXPERIMENTs 2 and 3 require numerical procedures to obtain the Markov chain's equilibrium distribution and thus the desired performance measures, equivalent measures for the single-BTS EXPERIMENTs 0, 1A and 1B can be obtained in closed-form. The model of EXPERIMENT 1B is an $M/G/1/PS/a_{\max}$ queueing model with state-dependent aggregate service rates given by $a\beta\left(a\right) \equiv \left(1-P_1\left(a\right)\right)R_{\text{DSCH}}$, $a = 1,\cdots,a_{\max}$. Of primary interest are the (conditional) expected transfer time $\mathbf{T}^\circ$ $(\mathbf{T}^\circ\left(x\right))$, which for the $M/G/1/PS/a_{\max}$ model is given by

$$\mathbf{T}^\circ\left(x\right) \equiv x\sum_{a=0}^{a_{\max}} \frac{a\,\pi\left(a\right)}{\rho\left(1-\mathbf{P}^{\mathcal{G}}\right)\left(1-\pi\left(a_{\max}\right)\right)} \quad \text{and} \quad \mathbf{T}^\circ \equiv \sum_{a=0}^{a_{\max}} \frac{a\,\pi\left(a\right)}{\lambda\left(1-\mathbf{P}^{\mathcal{G}}\right)\left(1-\pi\left(a_{\max}\right)\right)},$$

where

$$\pi\left(a\right) = \frac{\left(\rho\left(1-\mathbf{P}^{\mathcal{G}}\right)\right)^a \varphi_a}{\sum_{a'=0}^{a_{\max}}\left(\rho\left(1-\mathbf{P}^{\mathcal{G}}\right)\right)^{a'}\varphi_{a'}} \quad \text{with} \quad \varphi_a \equiv \left(\prod_{a'=1}^{a} a'\beta\left(a'\right)\right)^{-1},$$

$a = 0,\cdots,a_{\max}$, is the model's equilibrium distribution. These expressions have been shown to be insensitive to the data call size distribution except for its mean [6]. The models of EXPERIMENTs 0 and 1A are instances of the basic $M/G/1/PS/a_{\max}$ queueing model with fixed aggregate service rates $a\beta\left(a\right)$ equal to R_{DSCH} and $\left(1-P_b^\star\left(1\right)\right)R_{\text{DSCH}}$, respectively, and are thus special cases of the above-mentioned queueing model used to analyse EXPERIMENT 1B.

6 NUMERICAL RESULTS

Following the evaluation approach outlined in Section 4, a number of insightful numerical experiments are now presented to assess the 'round robin effect' and the different 'interference effects' caused by the DSCH's self-interference, the presence of A-DCHs and the influence from adjacent BTSs. Furthermore, the impact of the downlink orthogonality factor ω and the (uniform) traffic load $\rho_b = \rho$, $b \in \mathbb{B}$, is determined. The assumed parameter settings are summarised in Table 1 below. The values given for the maximum transmission power $p_{\max}$ and thermal noise level ν correspond to 42 dBm and -99.157 dBm^2, respectively. The assumed hexagonal cell radius of $R = 1/\sqrt{3} \approx 0.577$ km corresponds to an inter-BTS distance of precisely 1 km. The downlink orthogonality factors are taken from [7] ($\omega = 0.06$, indoor office test environment) and [20] ($\omega = 0.65$, typical urban channel) in order to consider two very distinct yet realistic alternatives.

SYSTEM MODEL			INTERFERENCE MODEL			TRAFFIC MODEL		
B	$\in \{1,2,3\}$	BTSs	η_{basic}	137.744	dB	μ^{-1}	320	kbits
R	$1/\sqrt{3}$	km	ς	3.523	-	λ	$\in [0, 2\mu R_{\text{DSCH}}]$	call/s
R_{CHIP}	3840	kchips/s	a	$1/\sqrt{2}$	-	$a_{\max}$	17	calls
R_{DSCH}	1024	kbits/s	b	$1/\sqrt{2}$	-			
γ_{DSCH}	4	dB	σ_{S}	8	dB			
$R_{\text{A-DCH}}$	3.4	kbits/s	ω	$\in \{0.06, 0.65\}$	-			
$\gamma_{\text{A-DCH}}$	7	dB	ν	$1.214\ 10^{-13}$	Watt			
$p_{\max}$	15.849	Watt						

Table 1: *Parameter settings.*

As with the performance analysis, the numerical experiments are presented in two separate stages.

STAGE I: INTERFERENCE ASPECTS

The objective of STAGE I is to determine the set of outage probability functions $\left\{P_b(\mathbf{a}),\ \mathbf{a} \in \mathbb{S}_b^+,\ b \in \mathbb{B}\right\}$, conditional on the path gain-based CAC criterion, by means of Monte Carlo simulations. The number of snapshots was taken to be $K = 100000$ to ensure that the relative precision of the constructed 95% confidence intervals is no worse than 3%. Consider first EXPERIMENTs 2 and 3. Given the network symmetry implied by the choice of $B \in \{2,3\}$ (see e.g. Figure 1), it holds that

$$\begin{cases} P_1(a_1,a_2) = P_2(a_2,a_1) & \text{for } B=2, \\ P_1(a_1,a_2,a_3) = P_2(a_2,a_1,a_3) = P_3(a_3,a_1,a_2) & \text{for } B=3, \end{cases}$$

and hence it suffices to determine only $\left\{P_1(\mathbf{a}),\ \mathbf{a} \in \mathbb{S}_1^+\right\}$.

For $B = 2$, $R_{\text{DSCH}} = 1024$ and $\omega \in \{0.06, 0.65\}$, Figure 3 shows the outage probability $P_1(\mathbf{a})$ as a function of $\mathbf{a} \in \mathbb{S}_1^+$. The accompanying Figure 4 shows the same numerical results but now in the form of iso-outage curves, a representation that may be useful to determine an appropriate CAC region. Aside from the trivial observation that $P_1(\mathbf{a})$ is increasing in both a_1 and a_2, the figure allows some additional insightful observations. There is a significant increase in $P_1(\mathbf{a})$ from $a_2 = 0$ to $a_2 = 1$, due to the activation of the DSCH in the adjacent cell, whose high data rate and the correspondingly low processing gain, requires a high transmission power and thus induces a large increase in the interference level experienced in the reference cell. In Figure 4 this sudden increase is apparent from the iso-outage curves' near alignment with the horizontal axes. As a_2 becomes larger, $P_1(\mathbf{a})$ increases with a much less dramatic (slightly positive) slope, since the raised interference is now only caused

[2] The effective thermal noise level ν equals $R_{\text{CHIP}} \cdot k \cdot T \cdot N_f$, where $R_{\text{CHIP}} = 3840$ kchips/s, $k \approx 1.38\,10^{-23}$ J/K is Boltzmann's constant, $T = 290$ K is the considered absolute temperature and $N_f = 9$ dB is the assumed receiver noise figure (see e.g. [13]).

by the additional low data rate A-DCHs, requiring relatively low transmission power levels. Comparing both charts, note that for $\omega = 0.65$, $P_1(\mathbf{a})$ shows a much greater dependency on a_1, due to the smaller orthogonality gain in the reference cell. As a consequence, the relatively high transmission powers thus required for greater a_1 and the resulting interference levels induce higher transmission powers at BTS 2, establishing an increasing dependency between both BTSs. Although this effect is present in both charts, it is particularly visible in the chart for $\omega = 0.65$.

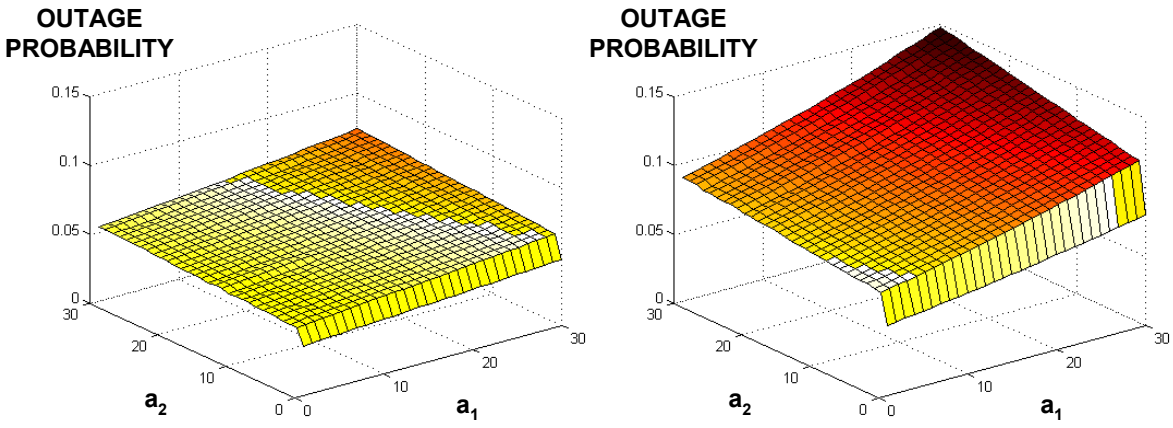

Figure 3: *Outage probabilities for* EXPERIMENT 2 *(left:* $\omega = 0.06$*; right:* $\omega = 0.65$*).*

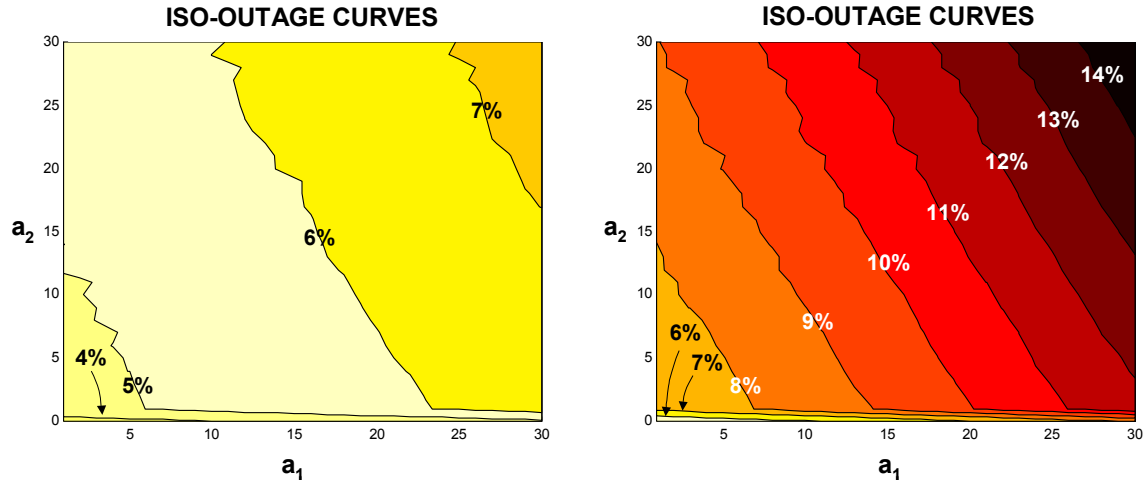

Figure 4: *Outage probabilities for* EXPERIMENT 2 *(left:* $\omega = 0.06$*; right:* $\omega = 0.65$*).*

With regards to the absolute values of the outage probabilities, note that for $\omega = 0.06$ (0.65), $P_1(\mathbf{a})$ varies between 0.0360 (0.0510) for $\mathbf{a} = (1, 0)$ and 0.0744 (0.1477) for $\mathbf{a} = (30, 30)$. As a visual presentation of the outage probabilities is not possible for $B = 3$, it is noted for comparison that in a network of three cells $P_1(\mathbf{a})$ varies between 0.0343 (0.0497) for $\mathbf{a} = (1, 0, 0)$ and 0.1015 (0.2230) for $\mathbf{a} = (30, 30, 30)$, for downlink orthogonality factor $\omega = 0.06$ (0.65). Observe that $P_1(1, 0, 0)$ $(B = 3)$ is slightly lower than $P_1(1, 0)$ $(B = 2)$ since the additional BTS may relieve BTS 1 of unfavourably (e.g. due to shadowing) located terminals (enhanced diversity gain), rather than allowing a poor QOS for the unfortunate call. Trivially, $P_1(30, 30, 30)$ $(B = 3)$ exceeds $P_1(30, 30)$ $(B = 2)$ significantly, due to the additional interference caused by BTS 3's DSCH and A-DCHs.

The outage probabilities for EXPERIMENTS 1A and 1B are given in Figure 5. Observe that in EXPERIMENT 1B, $P_1(1)$ is equal to 0.0373 (0.0524) for $\omega = 0.06$ (0.65), which implies that even in a single cell case serving a single randomly located data call, a DSCH at a rate of 1 Mbits/s may suffer a significant expected outage probability (or FER), due to the interference generated by the single A-DCH and the lack of perfect signal or-

thogonality due to multipath fading. In comparison with the corresponding values obtained for the experiments *with* A-DCHs, the outage probability $P_1^{\star}(1)$ for EXPERIMENT 1A (*without* A-DCHs) is slightly lower due to the reduced interference levels. The above-mentioned diversity gain observed in larger networks, induces that e.g. $P_1(a_1,0,0) < P_1(a_1,0) < P_1(a_1)$, $a_1 = 1,2,\cdots,a_{\max}$ (EXPERIMENTS 3, 2, 1B).

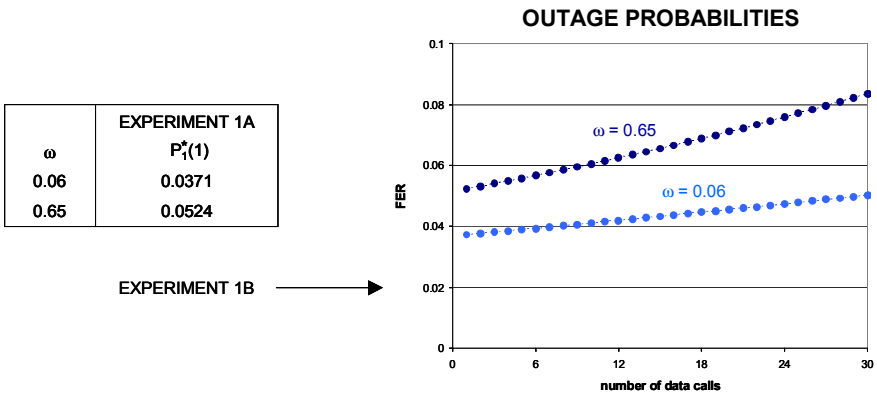

Figure 5: *Outage probabilities for* EXPERIMENTS 1A *(left) and* 1B *(right).*

As the STAGE I Monte Carlo simulations are used to derive an outage probability function, *conditional* on the compliance with the path gain-based CAC condition, the fraction of data calls $\mathbf{P}^{\mathcal{G}}$ that is rejected by this CAC scheme is also obtained. Table 2 contains $\mathbf{P}^{\mathcal{G}}$ for all considered experiments. Observe that $\mathbf{P}^{\mathcal{G}}$ increases in ω due to a reduced orthogonality gain, decreases in the number of BTSs due to an improved diversity gain, and increases slightly if the A-DCHs are included due to both the associated interference and the reduced BTS power budget that can be assigned to the actual DSCH transfer.

ω	EXPERIMENT 0	EXPERIMENT 1A	EXPERIMENT 1B	EXPERIMENT 2	EXPERIMENT 3
0.06	0.0000%	0.9380%	0.9475%	0.6814%	0.5342%
0.65	0.0000%	1.8658%	1.8927%	1.4450%	1.1784%

Table 2: *Fraction* $\mathbf{P}^{\mathcal{G}}$ *of data calls that is rejected due to the path gain-based* CAC *criterion.*

As stated above, the outage probability curves can be useful to derive secondary CAC threshold $a_{\max}$ and thus pose an upper bound on the outage probability. For the STAGE II experiments, we have assumed a typical outage requirement of less than 8%, which in a network of 3 BTSs and $\omega = 0.06$ implies a CAC threshold of $a_{\max} = 17$ (in a network of 1 (2) BTS(s) with the same multipath conditions this CAC threshold limits the outage probability to 4.42% (6.12%)). Whereas in practice, other CAC thresholds (possibly taking other BTSs' actual loading into account) may of course be set, depending on the specific propagation environment, the network size and the operator's policy, our qualitative comparisons require a uniform CAC threshold in all considered experiments.

STAGE II: TRAFFIC DYNAMICS

For each of the experiments, the required FER functions determined via Monte Carlo simulations in STAGE I are used to determine the state-dependent expected throughput in the STAGE II Markov chain model that captures the traffic dynamics. The performance analyses have been presented in Section 5 above.

For $R_{\text{DSCH}} = 1024$, $\omega \in \{0.06, 0.65\}$ and $\rho \in (0,2]$, Figure 6 shows the expected transfer times (in seconds) versus the data traffic load for all five experiments. At this point it is stressed that the traffic load definition is implicitly defined in terms of a uniform data call arrival rate λ for a *given* job size average μ^{-1}. While for EXPERIMENTS 0 and 1A the presented results are sensitive to λ and μ only through their ratio ρ, this is certainly

not the case for EXPERIMENTs 1B, 2 and 3, as in these experiments the *number* of present data calls affects the *aggregate* service rate due to the interference generated to maintain the A-DCHs.

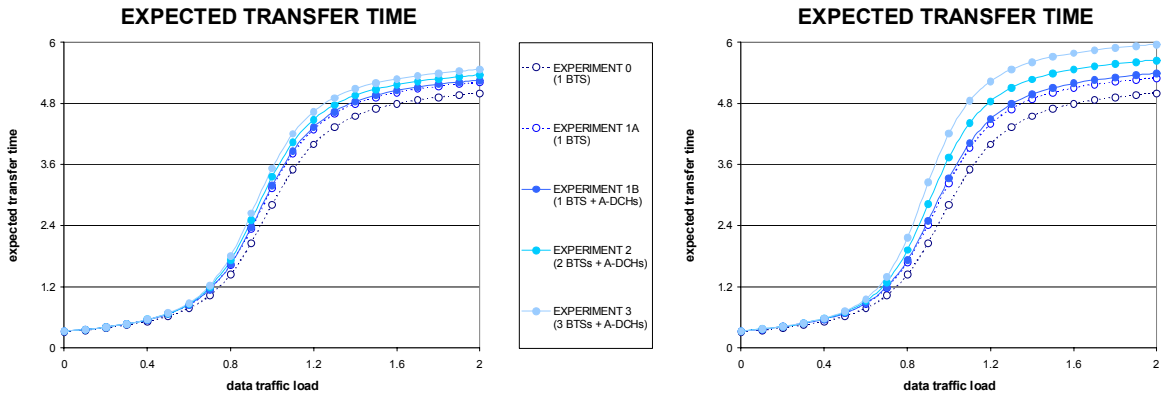

Figure 6: *Expected transfer times versus data traffic load, for* $\omega = 0.06$ *(left) and* $\omega = 0.65$ *(right).*

The general form of the curves shows an exponential QOS degradation for $\rho \in (0, 1]$, primarily due to the increase in the number of data calls sharing the DSCH resources, which is followed by a QOS stabilisation effectuated by the call admission control scheme ($a_{\max}$). It is the relative performance of the different experiments and downlink orthogonality factors that is of principal interest. In order to assess the different 'interference effects', the lower curve (EXPERIMENT 0) serves as a reference for the other curves as it represents the most basic scenario (capturing the 'round robin effect' only). For both values of ω, observe that in the single cell case the overall interference effect is captured for the better part by EXPERIMENT 1A, indicating that the inclusion of path gain-based CAC, the impact of the power budget limitation and primarily the DSCH's self-interference to the reference case, is substantially more significant than the further inclusion of the A-DCHs in EXPERIMENT 1B.

An extension of the system with additional BTSs in EXPERIMENTs 2 and 3 induces a further significant QOS degradation. Apparently (and expectedly), the raised interference levels due to the extra DSCH(S) and A-DCHs outweighs the enhanced diversity gain. Concentrating on the influence of ω, observe that not only the *absolute* QOS is worsened by a smaller degree of orthogonality (higher ω), but also the *relative* QOS degradation due to the addition of extra BTSs, is largest for the case of $\omega = 0.65$, even though a low ω indicates a *relatively* large intercellular interference contribution. Apparently, the fact that, in a myopic sense, a higher ω leads to higher transmission powers within each cell separately, outweighs the relatively small intercellular interference coupling. Although this is not demonstrated, it is important to remark that the admission control threshold $a_{\max}$ may also strongly influence the relative interference impact of the DSCHs and A-DCHs in adjacent cells. For instance, a more stringent call admission control (lower $a_{\max}$) reduces both the impact of the A-DCHs and the activity level of the DSCHs.

Figure 7 presents the conditional expected transfer time of a data call of size $x \in (0, 500]$ kbits for $\rho = 1$. While the graphs for EXPERIMENTS 0, 1A and 1B are straight lines, those for EXPERIMENTS 2 and 3 are slightly concave (see also [18, 21]) due to the random variations in the effective aggregate DSCH throughput caused by the dynamics in adjacent cells. Observe that the ordering of the curves corresponding to the different experiments agrees with those in Figure 6 (for $\rho = 1$), while the impact of ω on the relative performance of the different experiments is also similar. As the different curves are (approximately) straight lines, the transfer time 'mark-up' of the different model extensions incorporated in the experiments is (approximately) constant in the data file size x. For instance, for $\omega = 0.65$, the conditional expected transfer times in EXPERIMENTS 1A, 1B, 2 and 3, are approximately 15.30%, 18.67%, 37.28% and 49.30% higher, respectively, than those in EXPERIMENT 0.

The numerical section concludes with a comparison of the results obtained using the semi-analytical two-stage approach and those obtained by means of direct time-consuming dynamic simulations of the considered

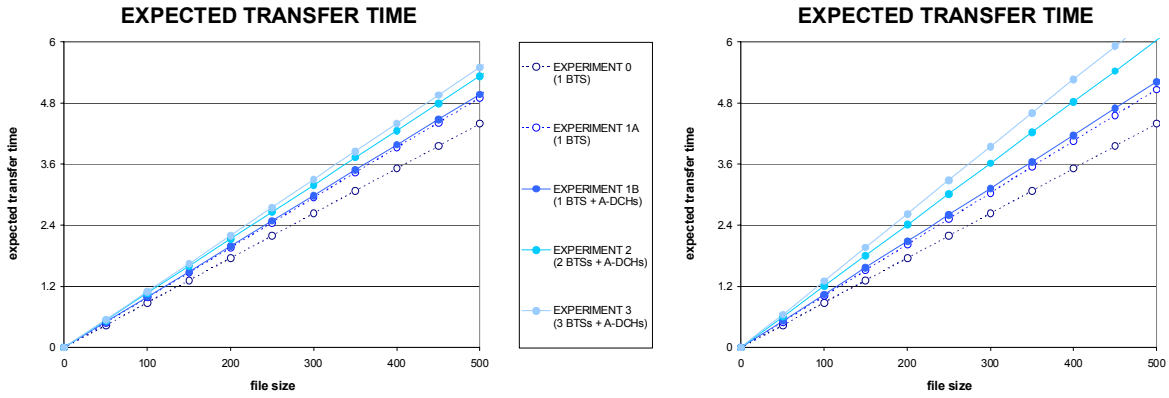

Figure 7: *Conditional expected transfer times versus data file size, for* $\omega = 0.06$ *(left) and* $\omega = 0.65$ *(right).*

system. Figure 8 (left) shows the expected transfer time curves for the case of $\omega = 0.65$. Note that the curve associated with EXPERIMENT 0 is identical to the corresponding curves in Figure 6. Observe first that the absolute QOS levels obtained in the simulation experiments are worse than the corresponding analytically obtained values. Three distinct causes can be identified for this discrepancy. *(i)* The simulations are run with a fixed 10 ms (UMTS time frame) heartbeat which typically requires padding of each call's final data frame and thus corresponds with a waste of capacity. *(ii)* The second stage in the analytical approach basically assumes all terminals to have an 'average location', whereas the dynamic simulations actually take the location variability into account by randomly sampling the location corresponding to each generated data call. *(iii)* The analytical approach implicitly assumes all competing data calls to be homogeneously distributed over the corresponding cells. However, the simulation results in Figure 8 (right) show that while the arrival process is spatially homogeneous, the spatial distribution of the calls present at any given time is typically skewed, due to the phenomenon that a data call nearer to its serving BTS experiences fewer frame errors and thus sooner completes its intended transfer and departs from the system. As the chart shows, this effect occurs even for a negligible traffic load, since a BTS's power budget may be insufficient to overpower the thermal noise level and self-interference at a remote terminal receiver in the presence of highly variable Rayleigh fading. The impact of the spatial inhomogeneity increases both under heavier data traffic loads and with the presence of (additional) DSCHs/A-DCHs, as the interference caused by the latter affects remote data calls most significantly.

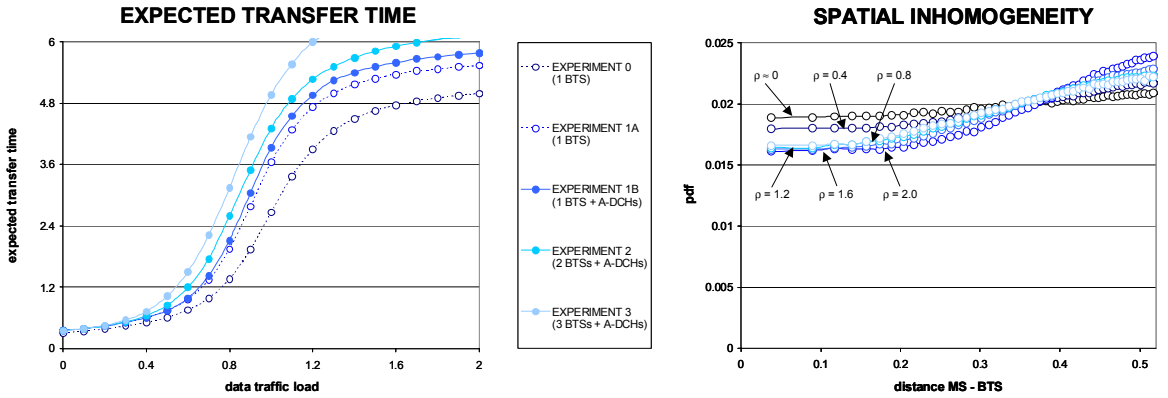

Figure 8: *Dynamic simulation results: expected transfer times versus data traffic load for* $\omega = 0.65$ *(left); illustration of induced spatial inhomogeneity (right).*

Aside from these absolute discrepancies, observe that the *qualitative* trends of the semi-analytical approach appear to be in line with those indicated by the simulation results (see Figure 6 (right)).

7 CONCLUDING REMARKS

We have presented a semi-analytical performance analysis of data transfer over Downlink Shared CHannels in UMTS networks. Following an insightful two-stage approach to segregate the interference aspects from the traffic dynamics, we have decomposed the general performance model into simpler experiments, in order to provide qualitative insight in the influence of different system aspects on the data QOS. In particular, the analysis has demonstrated that while *(i)* a heavier data traffic load implies a greater competition for DSCH resources and thus longer transfer delays ('round robin effect'); *(ii)* a heavier data traffic load also implies a higher interference level due to the greater number of A-DCHs that must be maintained for signalling purposes, which causes a higher frame error rate and thus a lower effective aggregate DSCH throughput ('interference effect'): *the greater the demand for service, the smaller the aggregate service capacity*. The principal advantages of the presented two-stage performance evaluation method are its relative swiftness, the benefits gained from the methods first stage, e.g. the possibility to derive CAC rules, and the delivered insight into the conditional data QOS given a file's size.

Among the observations from the presented numerical experiments, we note that the impact of the DSCHs' self-orthogonality on the data QOS dominates the impact of the interference from the A-DCHs thus validating the assumption often made in related publications (e.g. [3, 12, 15]) to disregard the A-DCHs. The results further illustrated that the raised interference caused by the inclusion of a(n additional) adjacent BTS leads to a QOS degradation that is slightly smaller than that caused by the inclusion of intra-cellular interference in a basic UMTS model. Although this is not numerically supported, the impact of including non-adjacent (e.g. second tier) BTSs is typically much smaller. The influence of the downlink orthogonality factor was demonstrated to be fairly significant, with lower degree of orthogonality leading to worse data QOS.

A comparison with direct dynamic simulations revealed that although absolute QOS levels differ, the principal *qualitative* purpose of the presented study is pleasingly backed. An important rationale behind the discrepancy in the absolute QOS performance between the presented semi-analytical approach and direct simulations, has been argued to be related to the spatial terminal distribution, which leads to some suggestions for further improvement of the considered model. For instance, it may prove fruitful to specify the terminal locations with a granularity finer than per cell, e.g. by partitioning each cell in (concentric) zones, which would effectively translate into a higher–dimensional state space. Other potentially fruitful approaches include an intelligent adjustment of the spatially uniform terminal distribution in the STAGE I Monte Carlo analysis, the application of a scheduling discipline which establishes the sort of fairness that preserves the spatially uniform terminal distribution (see also [15]) and modelling the spatial arrival/departure process in terms of geometries rather than (x, y) coordinates. As a final remark, we note that the presented two-stage approach for DSCH evaluations is readily extended to include different services and transport channels, for both up- and downlink.

References

[1] 3GPP TS 25.211, *"Physical channels and mapping of transport channels onto physical channels (FDD)"*, v3.5.0, Release 99, 2000.

[2] M. Andrews, K. Kumaran, K. Ramanan, A. Stolyar and P. Whiting, "Data rate scheduling algorithms and capacity estimates for the CDMA forward link", *Technical report BL0112120-990922-32TM,* Bell Labs, Lucent Technologies, USA, 1999.

[3] A. Bedekar, S.C. Borst, K. Ramanan, P.A. Whiting and M. Yeh, "Downlink scheduling in CDMA data networks", *Proceedings of IEEE Globecom '99,* Rio de Janeiro, Brazil, pp. 2653-2657, 1999.

[4] F. Berggren and S.-L. Kim, "Energy-efficient downlink power control and scheduling for CDMA non-real time data", *Proceedings of IEEE MMT '00,* Duck Key, USA, 2000.

[5] J.P. Castro, *"The UMTS network and radio access technology: air interface for future mobile systems"*, John Wiley & Sons, Chichester, England, 2001.

[6] J.W. Cohen, "The multiple phase network with generalized processor sharing", *Acta Informatica*, vol. 12, pp. 245-284, 1979.

[7] ETSI UMTS 30.04, *"UMTS terrestrial radio access; concept evaluation"*, ETSI, France, 1997.

[8] J.S. Evans and D.Everitt, "Effective bandwidth-based admission control for multi-service CDMA cellular networks", *IEEE Transactions on Vehicular Technology*, vol. 48, no. 1, pp. 36-46, 1999.

[9] K.W. Helmersson and G. Bark, "Performance of downlink shared channels in WCDMA radio networks", *Proceedings of IEEE VTC '01,* Rhodes, Greece, 2001.

[10] H. Holma and A. Toskala, *"WCDMA for UMTS: radio access for third generation mobile communications"*, John Wiley & Sons, Chichester, England, 2001.

[11] N. Joshi, S.R. Kadaba, S. Patel and G.S. Sundaram, "Downlink scheduling in CDMA data networks", *Proceedings of ACM/IEEE MOBICOM '00,* Boston, USA, pp. 179-190, 2000.

[12] K. Kumaran and P. Whiting, "Rate processor sharing: a robust technique for scheduling data transmissions in CDMA wireless networks", *Proceedings of Multiaccess Mobility and Teletraffic for Wireless Communications,* Venice, Italy, 1999.

[13] W.C.Y. Lee,. *"Mobile communications design fundamentals"*, Howard W. Sams & Co., Indianapolis, USA, 1986.

[14] R. Litjens, "The impact of mobility on UMTS network planning", *Computer networks,* vol. 38, no. 4, 2002.

[15] R. Litjens and J.L. van den Berg, "Fair adaptive scheduling in integrated services UMTS networks", *submitted for publication.*

[16] R. Litjens and J.L. van den Berg, "Performance analysis of adaptive scheduling in integrated services UMTS networks", *Proceedings of IEEE MWCN '02,* Stockholm, Sweden, pp. 3-7, 2002.

[17] R. Litjens and R.J. Boucherie, "Quality-of-service differentiation in an integrated services GSM/GPRS network", *submitted for publication,* 2001.

[18] R. Litjens and R.J. Boucherie, "Elastic calls in an integrated services network: the greater the call size variability the better the QOS", to appear in *Performance evaluation.*

[19] I. López, P.J. Ameigeiras, J. Wigard and P. Mogensen, "Downlink radio resource management for IP packet services in UMTS", *Proceedings of IEEE VTC '01,* Rhodes, Greece, 2001.

[20] N. B. Mehta, L. Greenstein, T. Willis and Z. Kostic, "Analysis and results for the orthogonality factor in WCDMA downlinks", *Proceedings of IEEE VTC '02,* Birmingham, USA, 2002.

[21] R. Núñez Queija, "Sojourn times in non-homogeneous QBD processes with processor sharing", *Stochastic models,* vol. 17, pp. 61-92, 2001.

[22] H.C. Tijms, *"Stochastic modelling and analysis: a computational approach"*, John Wiley & Sons, Chichester, England, 1986.

[23] A.J. Viterbi, *"CDMA: principles of spread spectrum communication"*, Addison-Wesley, Reading, USA, 1995.

[24] R.W. Wolff, *"Stochastic modeling and the theory of queues"*, Prentice-Hall, Englewood Cliffs, USA, 1989.